Title

Reactive Simulations of Silica Functionalization with Aromatic Hydrocarbons

Authors

Romero Garcia, Sergio
Zholdassov, Yerzhan S
Braunschweig, Adam B
et al.

Publication Date

2023-12-20

DOI

10.1021/acs.langmuir.3c02785

Reactive Simulations of Silica Functionalization with Aromatic Hydrocarbons

Sergio Romero Garcia,[†] Yerzhan S. Zholdassov,[‡,¶,§] Adam B. Braunschweig,[‡,¶,§] and Ashlie Martini[*,‖]

†*Department of Materials and Biomaterials Science and Engineering, University of California Merced, 5200 N. Lake Road, Merced, California 95343, United States*

‡*The Advanced Science Research Center at the Graduate Center of the City University of New York, 85 St. Nicholas Terrace, New York, New York 10031, USA*

¶*Department of Chemistry, Hunter College, 695 Park Avenue, New York, New York 10065, USA*

§*The Ph.D. Program in Chemistry, Graduate Center of the City University of New York, 365 Fifth Avenue, New York, New York 10016, USA*

‖*Department of Mechanical Engineering, University of California Merced, 5200 N. Lake Road, Merced, California 95343, United States*

E-mail: amartini@ucmerced.edu

Phone: +1 (209) 228-2354

Abstract

Reactive molecular dynamics simulations are used to model covalent functionalization of amorphous silica with aromatic hydrocarbons. Simulations show that the surface density of silanol-terminated phenyl, naphthyl, and anthracenyl molecules is lower than the maximum value calculated based on molecule geometry and the simulation densities decrease faster with number of aromatic rings than the geometric densities. The trends are analyzed in terms of the surface-silanol bonding configurations, tilt angles, local conformational ordering, and aggregation of surface-bound molecules in steady-state conditions. Results show that surface density is affected by both the size and symmetry of the aromatic hydrocarbons. The correlations between bonding, orientation, and surface density identified here may guide selection or design of molecules for functionalized surfaces.

Introduction

Modification of silica surfaces with organic molecules is important for the development of medical, electronic, and pharmaceutical applications. Chemical bonds that form between a silica substrate and organic molecules modify the chemical and physical properties of the surface.[1] This opens the possibility to control or tailor properties such as friction,[2] biocompatibility,[3] and polarity[4] to a specific application. Examples include functionalization of atomic force microscope tips to improve their useful life,[5] design of biocompatible amorphous silica[6] in drug delivery systems and implant applications[7] to treat osteoporotic fractures[8] and bone tumours or infections,[9] development of sensors for detecting biological analytes,[10] and creation of stimuli-responsive surfaces.[11]

Many different organic molecules have been immobilized on silica through the formation of new covalent bonds with the surface.[12] Among these, aromatic hydrocarbons (AH) have been used in solution-based and mechanochemically driven perycyclic reactions[13] and proposed for applications in organic electronic devices.[14] AH are composed of aromatic carbon rings, with those in the acene group made up of linearly bonded rings. In solution-based chemistry, functionalizing silica with AHs is possible at room temperature.[12] However, to further the development of AH silica functionalization as a predictable method to control surface properties, the mechanisms underlying chemical bond formation between the AH molecules and silica surface must be understood.

Importantly, chemical bonding affects the density of organic molecules on the surface which, in turn, determines the properties of the functionalized surface.[15] Observations of the change in contact angle of aromatic-modified substrates suggested surface density is affected by the orientation and size of the deposited molecules.[16] Studies of the surface properties of heterogenous polycyclic AH clusters[17] in soot showed that the surface densities of carbon atoms in solid-like configurations was affected by the structure of the surface-bound molecules, with smaller molecules, such as pyrene, contributing significantly to the surface density. Further, previous experiments showed that the adsorption of organic molecules with different functional groups on silica can be favored by molecular flexibility and good steric access of the adsorption active groups to the silica surface.[18]

Surface density can be estimated based on the geometry of a given molecule or measured using a quartz crystal microbalance (QCM).[19,20] Specific to the QCM method, by estimating the monolayer mass of the deposited molecules is possible to measure surface density. However, this method does not provide insight into the underlying chemical and physical processes and, particularly, the effect of the structure of the deposited molecules. Computational methods can provide complementary information about molecule and surface interactions at the atomic level. Some studies have used *ab initio* methods[7,21] for this purpose. However, the scaling of quantum calculations (i.e., $O(N^3_{electrons})$) makes such calculations unsuitable for modeling systems larger than a thousand atoms. In contrast, classical molecular dynamics (MD) simulations based on empirical potentials are more efficient as they scale with the number of atoms in the system (i.e., $O(N_{atoms})$).

The development of empirical potentials that model chemical reactions, such as ReaxFF,[22] has made it possible to observe bond formation in a dynamic simulation. The ReaxFF potential has been shown to accurately describe the geometry, stability, and chemical bonding of conjugate, non-conjugate, and radical-containing compounds.[23] Relevant to our current investigation, ReaxFF simulations have been used to study the formation of alkysilane self-assembled monolayers on silica[24] and shear-activated oxidative chemisorption and oligomerization of cyclic hydrocarbons on amorphous silica.[25,26] Simulations of the functionalization of crystalline silicon surfaces with alkyl radicals were able to accurately reproduce surface densities measured experimentally.[27]

In our previous work,[28] a method to simulate the functionalization of amorphous silica with 9-anthracenyltrimethoxysilane was developed to corroborate the surface density obtained from experimental solution-based depositions. In experiments, the packing of AH monolayers is controlled by using a closed saturated solvent environment[29] (e.g. PhMe) that promotes reactions between the hydroxylated substrate and the silane-methyl terminated AH molecule. This opens oxygen reactive sites for the now silanol termination on the AH molecules to form covalent bonds with the surface. To focus on the covalent bonding of molecules to the substrate and improve simulation times, the simulations were performed using a model system in which the silica was dehydroxylated and the depositing molecules were AH terminated by a dehydroxylated silanol group, subsequently referred to simply as silanols in this manuscript. These simulations showed the time evolution of surface density, where the simulated steady-state value was in agreement with density measured using QCM.[28] However, the study did not provide insight into the effect of silanol structure in surface density, which is key for the selection of chemical species for surface functionalization for a specific application.

Here, we expand on our previous work by using reactive MD simulations to understand the effect of molecular structure on the covalent functionalization of amorphous silica with silanols and, specifically, on surface density. We model the condensation reactions between silica and three silanols with different numbers of aromatic rings at three different temperatures. We compare simulation calculated densities with those estimated using simple geometric models based on van der Waals radii. Then, we analyze surface densities in terms of the type and number of covalent bonds formed with the amorphous silica and the orientation and ordering of the silanols, revealing correlations between surface density and local conformational ordering of the silanols on the silica surface.

Materials and Methods

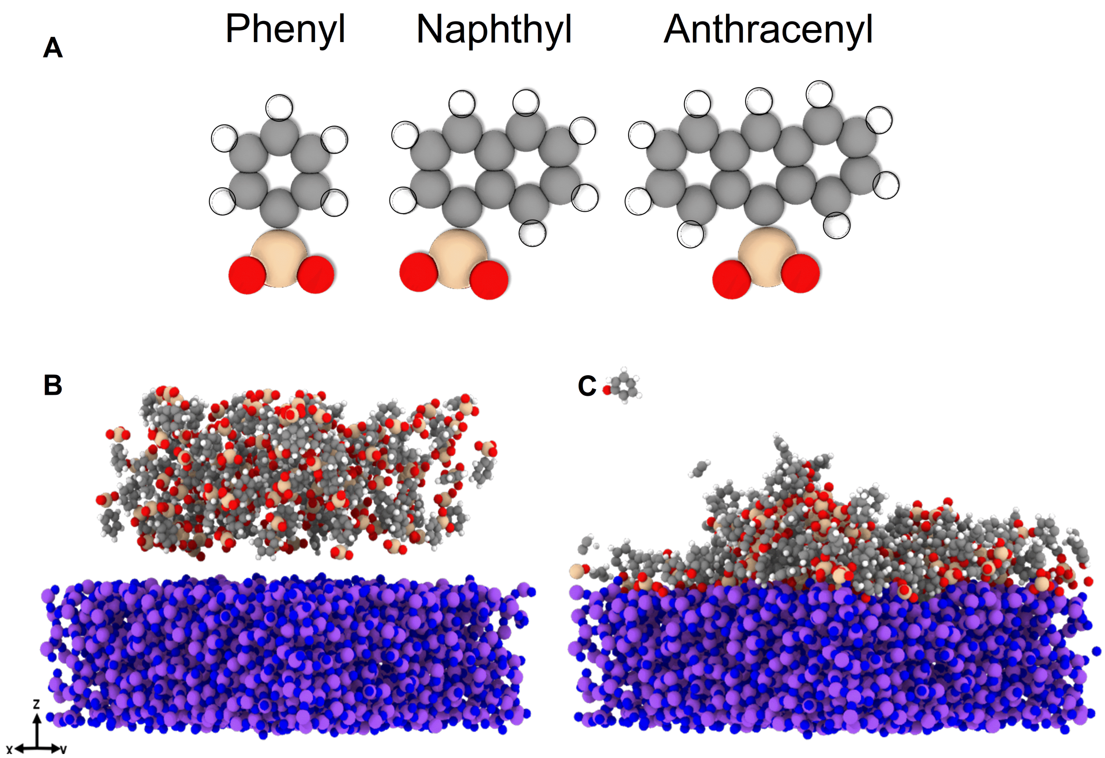

Figure 1: (A) Schematic representations of the aromatic hydrocarbons used as reactants in the simulations. Representative side-view snapshots of the model system with phenyl (B) before and (C) after covalent functionalization. Sphere colors correspond to: gray - carbon, white - hydrogen, tan - silicon in the silanols, purple - silicone in the silica, red - oxygen in the silanols, blue - oxygen in the silica.

The model system comprised a dehydroxylated silica substrate and aromatic hydrocarbons terminated by a dehydroxylated silanol group (silanols). This simplified model mimics the last step of reactions reported in our previous experimental study.[28] Specifically, in the experiments, a silica substrate was immersed in a PhMe solution containing 9-anthracenyltrimethoxysilane to initiate reactions between the methyl termination of the AH and the hydroxyl groups on the substrate surface. The reaction was assumed to proceed through initial steps to form dangling bonds on the substrate and AH, leading to chemical bonding between the $Si_{substrate}$ and O_{AH}. Therefore, we modeled only the last step, i.e., reaction between dehydroxylated silica and dehydroxylated silanols, to maximize the number of reactions of interest within the size and time-scale limitations of the reactive MD method.

The amorphous SiO_2 was generated from a cristobalite SiO_2 crystal structure[30] that was heated (5000 K) and fast quenched (300 K) in a simulation box with periodic boundary conditions in all directions and dimensions 5.6 × 6.0 × 2.1 nm (x, y, and z). The resulting amorphous structure exhibited Si-O, O-O, and Si-Si peaks and distances characterized by radial distribution functions (SI Fig. S1) that showed good agreement with values reported in literature for amorphous SiO_2 thin films.[31] Then, the dimensions of the box were extended to 5.6 × 6.0 × 5.5 nm (x, y, and z) to create a surface. The density of accessible dangling bonds on the equilibrated substrate surface before deposition was calculated to be 4.55 nm^{-2} with 153 open sites available for reaction.

Three silanols were modeled – phenyl, naphthyl, and anthracenyl – as shown in Fig. 1(A). The silanols were designed with the Avogadro chemical editor[32] and then placed randomly into the simulation box at a distance of at least 0.5 nm from the silica surface using PACKMOL.[33] Characterization of functionalized surface in the corresponding previous experiments suggested complete surface coverage.[28] Based on this, the number of silanols per simulation, 150, was determined as the approximate number needed to ensure full surface coverage within the short time-scale of the simulations. After this stage, the boundary conditions were periodic in x and y, while the z boundaries were fixed. The bottommost atoms in the silica slab were fixed during the simulation and a repulsive wall was used at the top of the simulation box to prevent silanols from escaping.

Reactive MD simulations were performed using the Large-scale Atomic/Molecular Massively Parallel Simulator (LAMMPS)[34] package. Atomic interactions were modeled with a time step of 0.1 fs using the ReaxFF potential for H/C/O/Si[35] parameterized to maintain thermal stability of C-Si bonds in silicon surfaces functionalized with organic molecules. Initial atom velocities were given by a Gaussian distribution at three different temperatures (300, 400, and 500 K). Simulations were run using the NVT ensemble (constant number of particles, volume, and temperature) using a Nosé-Hoover[36] thermostat with a damping parameter of 40 fs.

The simulations were run at each of the three temperatures for 0.2 ns, which was determined to be enough time for the surface reactions to reach steady state, as shown in SI Fig. S2. Snapshots of a representative model system before and after the dynamic simulations are shown in Fig. 1(B) and (C). Each simulation case was replicated three times using different random seed values for the initial atom velocities such that the repeat simulations were independent. Trajectory information was output every 5 ps and the bond table from ReaxFF that tracks the strength and number of covalent bonds was output every 0.2 ps. Visualization and analysis of atomic chemisorption from simulated data was done in OVITO[37] open-visualization tool and custom scripts written in Python.

Results and Discussion

During the simulations, chemical bonds formed between silicon in the silanols and oxygen on the silica surface. The number of silanols chemically bound to the surface was tracked (based on the formation of $Si_{silanol}$–O_{silica} bonds) and surface density was calculated from the number of surface-bound silanols divided by the silica surface area (32.9 nm^2). The time evolution of the surface density at each temperature for phenyl, naphthyl, and anthracenyl is shown in Fig. 2(A), (B), and (C), respectively. Bond formation occurred as soon as the simulation began and the surface density increased rapidly during the first 0.05 ns in all cases. The density reached a steady-state value after about 0.1 ns. At the end of the simulation, the silica surface was covered by a monolayer of chemically bound silanols, e.g., Fig. 1(C). The trajectories of the silanols were also tracked, showing that silanol movement on the surface was negligible after steady-state was reached (Figs. S4 and S5). Therefore, subsequent analyses focused on characterizing the bonding, conformation, and orientation of the surface-bound silanols between between 0.1 and 0.2 ns.

The steady-state surface density for each silanol and temperature averaged over three independent simulations is reported in Fig. 2(D). The results show that temperature did not have a statistically significant effect on surface density but the densities were very different for the three different silanols. Therefore, subsequent analyses focused on the silanols and included data from simulations at all three temperatures. The average steady-state surface density was 2.06 ± 0.12, 1.38 ± 0.15, and 1.15 ± 0.09 nm^{-2} for phenyl, naphthyl, and anthracenyl, respectively. The value for anthracenyl is comparable to surface density previously measured using QCM of 1.12 ± 0.13 nm^{-2}.[28] Further, the trend with respect to the three silanols is consistent with the expectation that the larger silanols should occupy more surface area therefore have lower density.

The maximum possible density for each silanol can be estimated based on the size of the molecules. Specifically, the van der Waals areas of the molecules[38] in the xy plane (visual representations in SI Fig. S3) were calculated to be 0.438, 0.582, and 0.720 nm^2, corresponding to maximum surface densities of 2.28, 1.71, and 1.38 nm^{-2} for phenyl, naphthyl, and anthracenyl, respectively. These values, as well as the densities obtained from simulations and reported from experiments, are given in Table 1. The simulation and experimental densities are lower than the maximum based on molecule geometry, which is reasonable since the maximum value assumes the silanols are ideally conformationally ordered, which is not expected to be the case in practice. The biggest difference between simulated and geometric density is for naphthyl. Also, the simulation densities decrease faster with increasing number of aromatic rings than the geometric densities. For example, the ratio of the theoretical densities of anthracenyl and phenyl is 1.65 but was found to be 1.79 ± 0.175 in the simulations.

Table 1: Summary of surface density values estimated based on molecule geometry, reactive MD simulations, and previous QCM measurements[28]

	Surface Density (nm^{-2})		
Method	Phenyl	Naphthyl	Anthracenyl
Geometric Maximum	2.28	1.71	1.38
MD Simulations	2.06 ± 0.12	1.38 ± 0.15	1.15 ± 0.09
QCM Experiments	-	-	1.12 ± 0.13

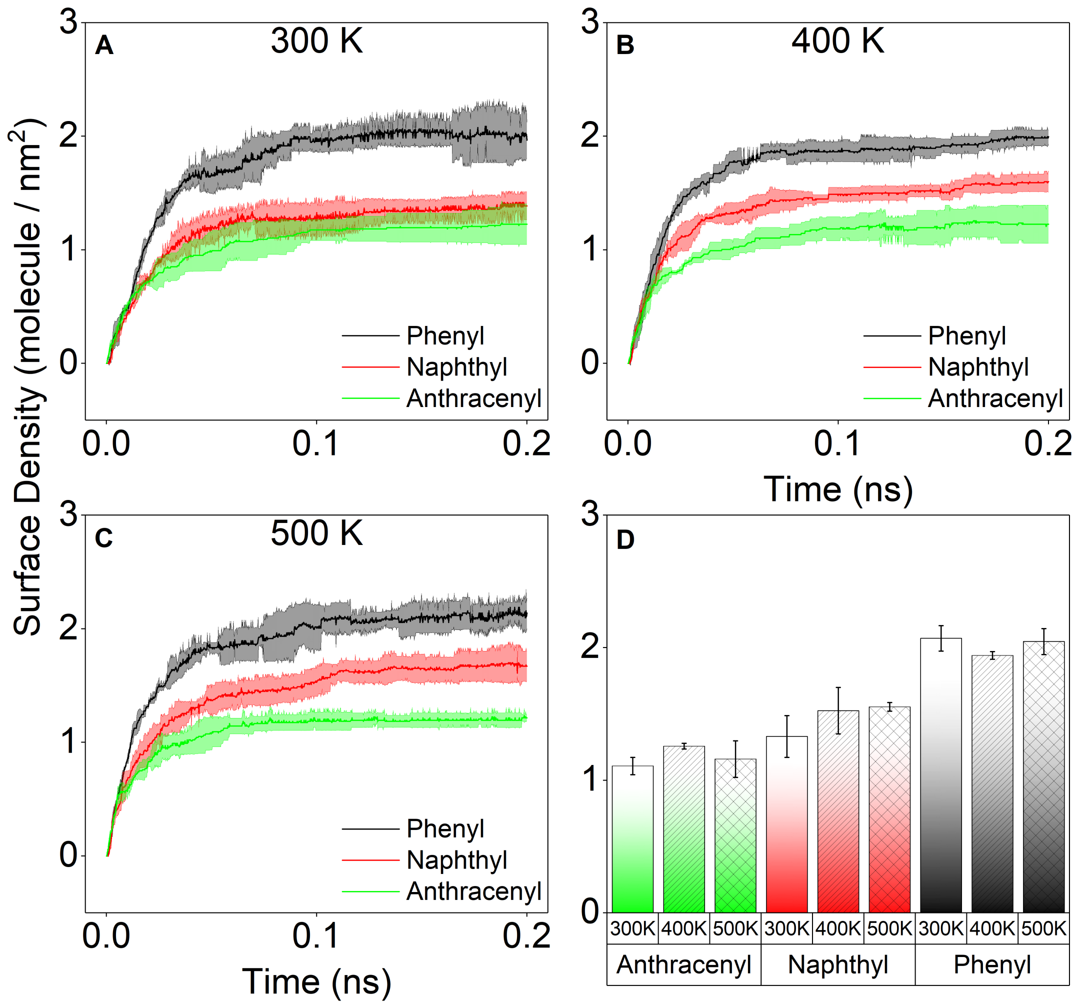

Figure 2: Time evolution of the surface density for phenyl, naphthyl, and anthracenyl chemisorbed on an amorphous silica surface from simulations at (A) 300, (B) 400, and (C) 500 K. For each data set, the dark line is the mean and the shaded region is the standard deviation of three independent simulations. (D) The steady-state surface density for each case is averaged over the last 0.1 ns of the simulations, where error bars reflect the standard deviation.

Analysis of anthracenyl chemisorption studied previously[28] showed that there are three types of bonding configurations possible, depending on how many silicon–oxygen bonds are formed, as illustrated in the close-up snapshots in Fig. 3(A), (B), and (C). Fig. 3(D) shows the distribution of bonding configurations for the surface-bound silanols, including data from all three simulated temperatures. The bond type distribution shows that the likelihood of a given configuration decreased with number of bonds. Specifically, for all silanols, one oxygen bond (1-O) was the most common and the least observed bonding configuration was three-oxygen (3-O) atoms. However, the statistical difference between 1-O and 2-O was smallest for naphthyl and the average percentage of 3-O was the largest for this silanol.

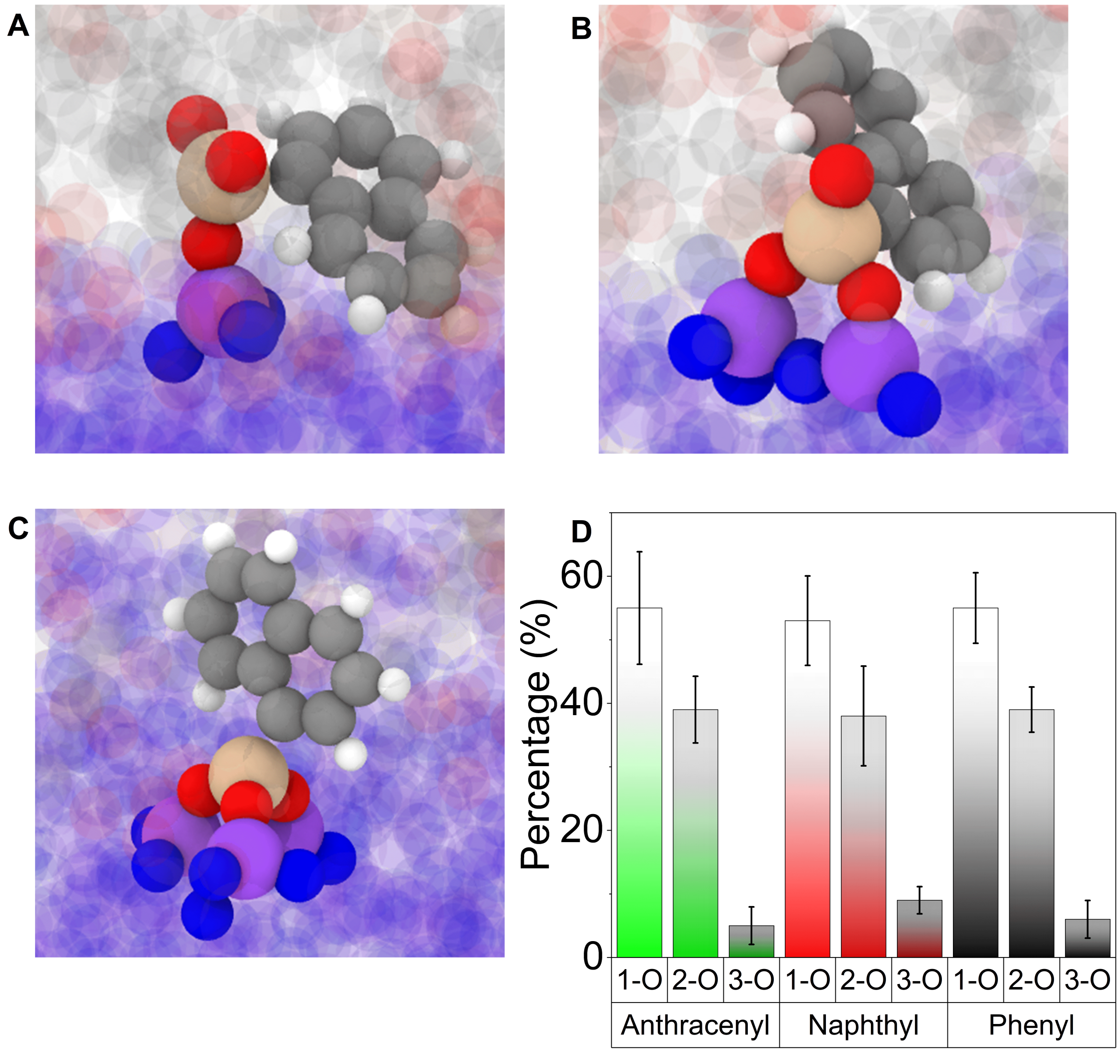

Figure 3: Close up snapshots of the three possible bonding configurations between a silanol and the silica substrate that differ based on the number of $Si_{silanol}$–O_{silica} bonds, shown using naphthyl as reference: (A) one bond (1-O), (B) two bonds (2-O), and (C) three bonds (3-O). Spheres representing atoms other than those in the representative silanols of interest are faded. (D) Distribution of the number of bonds between Si in the substrate and O in the silanol averaged over the three simulations at three temperatures for each silanol as a percentage of the total number of silanols in the system. The error bars represent the standard deviation.

Since the orientation of the surface-bound silanols can play a significant role in the properties of functionalized silica surfaces, the angle of tilt of the silanol with respect to the surface was analyzed. The tilt angle θ was defined as the angle between the plane of the ring(s) in the silanol and the direction normal to the silica surface, as shown in Fig. 4(A). The angle was calculated for each silanol bonded to the substrate using data from 0.1 to 0.2 ns of simulation time. The distributions of tilt angles in Figure 4(B) are positively skewed where the highest angle probability is 28.4° for all three silanols (distribution modes are $27.9 \pm 0.5°$, $28.7 \pm 0.6°$, and $30.3 \pm 0.8°$ for phenyl, naphthyl, and anthracenyl, respectively). This is consistent with the range of angles for self-assembled monolayers (SAM) on amorphous silica which have been reported to be 16° at full coverage[39] and as low as 30° for low coverage.[40] The highest angle probability of 28° for silanols in our study is at the upper end of the range reported for SAMs, consistent with the fact that our surface densities are below the geometric value (Table 1). Lastly, although the distributions are very similar for all three silanols, there are more small angles for the phenyl. This is consistent with a previous simulation-based study[41] of alkanethiol SAMs that reported tilt angle increased with chain length.

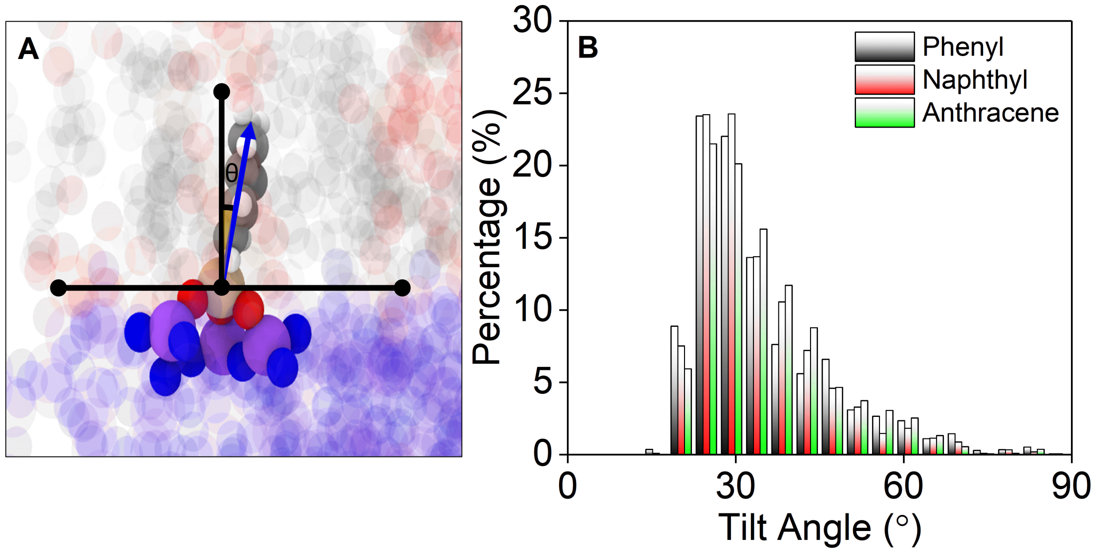

Figure 4: (A) Representative snapshot of phenyl showing the definition of the angle used to quantify the tilt of the silanol with respect to the surface-normal direction. Spheres representing atoms other than those in the representative silanol of interest are faded. (B) Distribution of tilt angles from all observed bonds and all temperatures/simulations between 0.1 and 0.2 ns of simulation time. Only slight differences between phenyl, naphthyl, and anthracenyl are observed, but smaller angles are preferred for the smaller silanols.

Another factor that can affect surface density of aromatic hydrocarbons is the orientation of molecules with respect to each other. Fig. 5(A), (B) and (C) shows two point vector representations of the surface-bound silanols in the xy plane for representative simulations. The vector is defined from the positions of the two edge carbon atoms on the long axis of the silanol, as shown in the Fig. 5 insets. Note that the arrows point only one direction for naphthyl to reflect the asymmetry of that silanol. The vectors are colored based on their angle with respect to the x-axis; the x-axis is an arbitrary direction but, if the silanols are conformationally ordered, there will be more arrows in Fig. 5(A), (B) and (C) with similar colors. This qualitative analysis shows some evidence of local ordering, but clearly the silanols are not ordered into the closest packed configuration assumed in the geometric density calculations (Fig. S3). This may be correlated to the preferential 1-O bonding exhibited by all three silanols in Fig. 3(D), since fewer chemical bonds enable more flexibility and rotation ability.

Next, we quantified the local ordering using radial distribution functions (RDFs)[41] of the distance between Si atoms in the surface-bound silanols for all the frames between 0.1 to 0.2 ns. The results for all simulations and temperatures are shown in Fig. 5(D), (E), and (F). If the silanols were ordered in their closest packed configuration, the smallest distance between silanols would be ≈0.3 nm. This is approximately where the first peak is seen in the RDFs in all three cases. However, there are also differences between the three silanols. Particularly, the first peak is broadest and shortest for phenyl, indicating these silanols are the least conformationally ordered. Less conformational ordering is associated with larger available volume for conformational changes, consistent with the smaller tilt angles for phenyl in Fig. 4(B).

The RDF peaks at farther distances reflect longer range ordering of the silanols. Interestingly, for phenyl and anthracenyl there are distinct peaks around 0.40, 0.47 and 0.55 nm, associated with preferred orientations of adjacent chemisorbed species. However, for naphthyl, the RDF peaks are broader and less distinct, indicating less long range order.

The naphthyl also had the least distinction between the different bonding configurations in Fig. 3(D) and the largest difference between the simulated and estimated surface densities in Table 1. The difference between naphthyl and the other two silanols is symmetry, with only naphthyl being asymmetric relative to the silicon atom. These results show that asymmetry decreases long-range order which, in turn, decreases the achievable surface density relative to the maximum possible value.

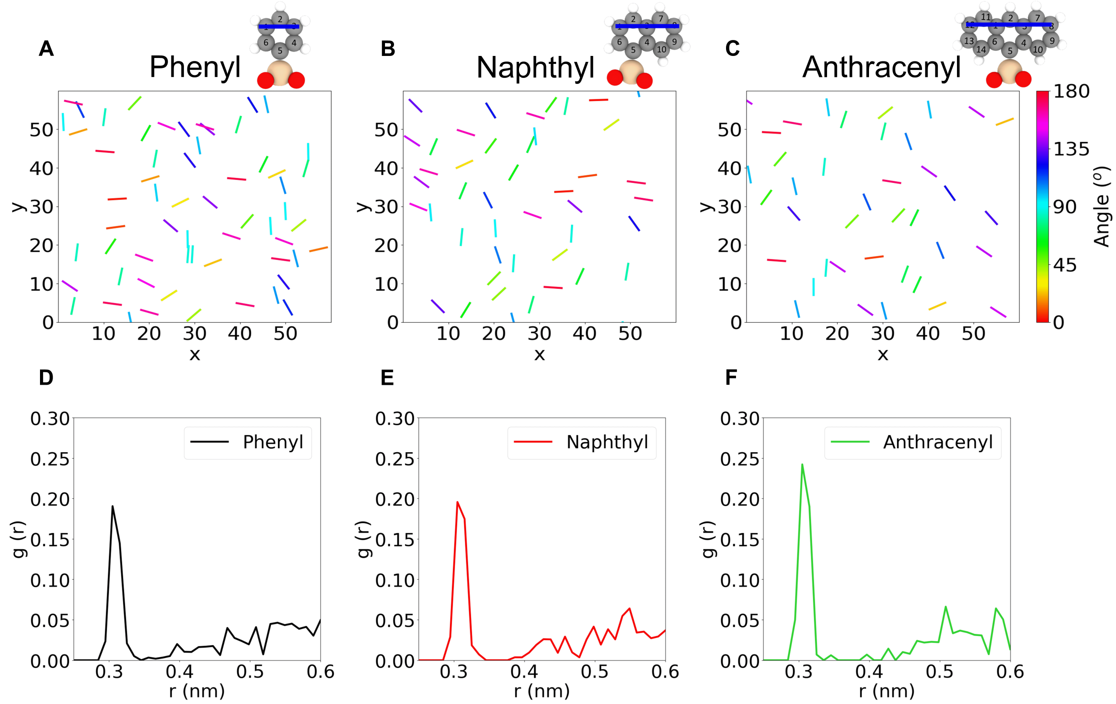

Figure 5: Two point vector representations of the silanol in the xy plane from representative simulations of (A) phenyl, (B) naphthyl, and (C) anthracenyl. The two point coordinates are taken from the edge carbons on the long axis of the silanol, as shown in the insets. The x- and y-axes are scaled by the total length of the simulation box in each direction. Radial distribution functions of the distance between Si atoms in (D) phenyl, (E) naphthyl, and (F) anthracenyl for all simulations.

Finally, surface density may be affected by the interaction and bonding between silanols resulting in aggregates.[42] An example is shown in Fig. 6(A), where two naphthyl molecules associate via an oxygen bond. This behavior was analyzed for all three silanols by calculating the distributions of aggregate size (e.g. 1-silanol, 2-silanol, 3-silanol, etc.) during steady-state, as shown in Fig. 6(B). The most commonly observed configuration is 1 silanol, meaning not aggregated. However, all three molecules form multiple dimers and trimers as well as even larger aggregates. Comparing the three silanols, anthracenyl has the fewest and smallest aggregates, while the phenyl has the most and largest aggregates. Since the association reactions always occur via an Si-O-Si bond, the trend observed in the aggregation results can be associated with molecular size and surface density, where larger silanols are further apart and less likely to aggregate.

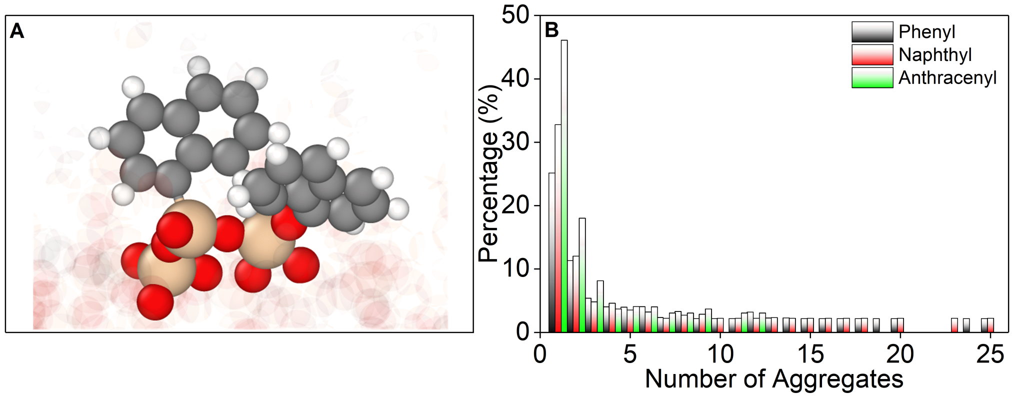

Figure 6: (A) Representative snapshot of a two-naphthl aggregate. (B) Distributions of aggregate size (quantified by number of bonded silanols) for each silanol calculated from trajectory data between 0.1 and 0.2 ns.

Conclusions

Reactive simulations were used to study the covalent functionalization of amorphous silica with silanol aromatic hydrocarbons. Surface density increased with decreasing molecular size, consistent with the maximum densities estimated from molecule geometry in a closest-packed configuration. The simulation densities were smaller than the estimated maximum values and the biggest difference between simulation and estimation was observed for naphthyl. Three possible chemical bonding configurations were observed and it was shown that all three silanols preferentially formed fewer covalent bonds, facilitating bending or rotation. Tilt angles were also calculated and shown to be smaller for smaller molecules. Local conformational ordering, analyzed qualitatively and quantitatively, was found to increase with molecule size. However, the least long-range order was exhibited by the asymmetric naphthyl silanol, a result that was correlated to the larger difference between the simulation and estimated surface density. Finally, analysis of aggregation of surface-bound species showed that smaller size and higher density were also associated with the formation of more and larger aggregates. These results show that both size and symmetry affect the surface density achievable in covalent functionalization of surfaces with silanol aromatic hydrocarbons. Future work using ab initio calculations may corroborate these findings and provide further insight into the structure-bonding relationship. Generally, these simulation-based approaches can inform our understanding of how molecular structure affects surface density which can guide the selection or design of molecules to achieve an ideal surface density and, in turn, ideal properties, for a specific surface or application.

Supporting Information Available

Radial distribution functions (RDFs) for the substrate Si-O, O-O; and Si-Si atom pairs before and after the amorphization step; surface density calculations from extended simulation run times for selected systems; schematic representation of the theoretical surface density calculations for each molecule type; and representative snapshots of silanol trajectories and mean square displacement of the silanol over time at different temperatures

Acknowledgement

Research performed as part of the Center of Mechanical Chemical Control supported by the Division of Chemistry of the National Science Foundation under grant #2023644. Simulations run on resources provided by the ACCESS advanced computing and data resource supported by the National Science Foundation.

References

(1) Barth, J. V.; Costantini, G.; Kern, K. Engineering atomic and molecular nanostructures at surfaces. *Nature* **2005**, *437*, 671–679.

(2) Sui, T.; Song, B.; Wen, Y.-H.; Zhang, F. Bifunctional hairy silica nanoparticles as high-performance additives for lubricant. *Sci. Rep.* **2016**, *6*, 22696.

(3) Zhang, S.; Niu, H.; Zhang, Y.; Liu, J.; Shi, Y.; Zhang, X.; Cai, Y. Biocompatible phosphatidylcholine bilayer coated on magnetic nanoparticles and their application in the extraction of several polycyclic aromatic hydrocarbons from environmental water and milk samples. *J. Chromatogr. A* **2012**, *1238*, 38–45.

(4) Filler, M. A.; Bent, S. F. The surface as molecular reagent: organic chemistry at the semiconductor interface. *Prog. Surf. Sci.* **2003**, *73*, 1–56.

(5) Berman, D.; Krim, J. Surface science, MEMS and NEMS: Progress and opportunities for surface science research performed on, or by, microdevices. *Prog. Surf. Sci.* **2013**, *88*, 171–211.

(6) Lai, C.-Y.; Trewyn, B. G.; Jeftinija, D. M.; Jeftinija, K.; Xu, S.; Jeftinija, S.; Lin, V. S.-Y. A mesoporous silica nanosphere-based carrier system with chemically removable CdS nanoparticle caps for stimuli-responsive controlled release of neurotransmitters and drug molecules. *J. Am. Chem. Soc.* **2003**, *125*, 4451–4459.

(7) Corno, M.; Delle Piane, M.; Choquet, P.; Ugliengo, P. Models for biomedical interfaces: a computational study of quinone-functionalized amorphous silica surface features. *Phys. Chem. Chem. Phys.* **2017**, *19*, 7793–7806.

(8) Ilyas, A.; Odatsu, T.; Shah, A.; Monte, F.; Kim, H. K. W.; Kramer, P.; Aswath, P. B.; Varanasi, V. G. Amorphous Silica: A New Antioxidant Role for Rapid Critical-Sized Bone Defect Healing. *Adv. Healthc. Mater.* **2016**, *5*, 2199–2213.

(9) Sayed, E.; Haj-Ahmad, R.; Ruparelia, K.; Arshad, M. S.; Chang, M.-W.; Ahmad, Z. Porous Inorganic Drug Delivery Systems-a Review. *AAPS PharmSciTech* **2017**, *18*, 1507–1525.

(10) Valles, D. J.; Zholdassov, Y. S.; Korpanty, J.; Uddin, S.; Naeem, Y.; Mootoo, D. R.; Gianneschi, N. C.; Braunschweig, A. B. Glycopolymer Microarrays with Sub-Femtomolar

Avidity for Glycan Binding Proteins Prepared by Grafted-To/Grafted-From Photopolymerizations. *Angew. Chem. Int. Ed Engl.* **2021**, *60*, 20350–20357.

(11) Zholdassov, Y. S.; Valles, D. J.; Uddin, S.; Korpanty, J.; Gianneschi, N. C.; Braunschweig, A. B. Orthogonal Images Concealed Within a Responsive 6-Dimensional Hypersurface. *Adv. Mater.* **2021**, *33*, e2100803.

(12) Rimola, A.; Costa, D.; Sodupe, M.; Lambert, J.-F.; Ugliengo, P. Silica surface features and their role in the adsorption of biomolecules: computational modeling and experiments. *Chem. Rev.* **2013**, *113*, 4216–4313.

(13) Sulkanen, A. R.; Sung, J.; Robb, M. J.; Moore, J. S.; Sottos, N. R.; Liu, G. Y. Spatially Selective and Density-Controlled Activation of Interfacial Mechanophores. *J. Am. Chem. Soc.* **2019**, *141*, 4080–4085.

(14) Tao, F. *Functionalization of semiconductor surfaces*; Wiley: Hoboken, NJ, 2012.

(15) Veerbeek, J.; Huskens, J. Applications of monolayer-functionalized H-terminated silicon surfaces: A review. *Small Methods* **2017**, *1*, 1700072.

(16) Hong, Y.; Chen, W.; Fang, H.; Zuo, B.; Yuan, Y.; Zhang, L.; Wang, X. Regulation of the Interfacial Effects of Thin Polystyrene Films by Changing the Aromatic Group Structure on Substrate Surfaces. *J. Phys. Chem. C* **2019**, *123*, 19715–19724.

(17) Bowal, K.; Pascazio, L.; Wang, H.; Chen, D.; Kraft, M. Surface properties of heterogeneous polycyclic aromatic hydrocarbon clusters. *Proc. Combust. Inst.* **2021**, *38*, 1115–1123.

(18) Diaz, L.; Liauw, C. M.; Edge, M.; Allen, N. S.; McMahon, A.; Rhodes, N. Investigation of factors affecting the adsorption of functional molecules onto gel silicas. 1. Flow microcalorimetry and infrared spectroscopy. *J. Colloid Interface Sci.* **2005**, *287*, 379–387.

(19) Stålgren, J. J. R.; Eriksson, J.; Boschkova, K. A comparative study of surfactant adsorption on model surfaces using the quartz crystal microbalance and the ellipsometer. *J. Colloid Interface Sci.* **2002**, *253*, 190–195.

(20) Sauerbrey, G. Verwendung von Schwingquarzen zur Wägung dünner Schichten und zur Mikrowägung. *Zeitschrift für Physik* **1959**, *155*, 206–222.

(21) Leftwich, T. R.; Madachik, M. R.; Teplyakov, A. V. Dehydrative cyclocondensation reactions on hydrogen-terminated Si(100) and Si(111): an ex situ tool for the modification of semiconductor surfaces. *J. Am. Chem. Soc.* **2008**, *130*, 16216–16223.

(22) van Duin, A. C. T.; Dasgupta, S.; Lorant, F.; Goddard, W. A. ReaxFF: A Reactive Force Field for Hydrocarbons. *J. Phys. Chem. A* **2001**, *105*, 9396–9409.

(23) Han, Y.; Jiang, D.; Zhang, J.; Li, W.; Gan, Z.; Gu, J. Development, applications and challenges of ReaxFF reactive force field in molecular simulations. *Frontiers of Chemical Science and Engineering* **2016**, *10*, 16–38.

(24) Black, J. E.; Iacovella, C. R.; Cummings, P. T.; McCabe, C. Molecular dynamics study of alkylsilane monolayers on realistic amorphous silica surfaces. *Langmuir* **2015**, *31*, 3086–3093.

(25) Bhuiyan, F. H.; Kim, S. H.; Martini, A. Reactive molecular dynamics simulations of thermal and shear-driven oligomerization. *Appl. Surf. Sci.* **2022**, *591*, 153209.

(26) Bhuiyan, F. H.; Li, Y.-S.; Kim, S. H.; Martini, A. Shear-activated chemisorption and association of cyclic organic molecules. *Faraday Discuss.* **2023**, *241*, 194–205.

(27) Soria, F. A.; Zhang, W.; Paredes-Olivera, P. A.; Van Duin, A. C. T.; Patrito, E. M. Si/C/H ReaxFF Reactive Potential for Silicon Surfaces Grafted with Organic Molecules. *J. Phys. Chem. C* **2018**, *122*, 23515–23527.

(28) Zholdassov, Y. S.; Yuan, L.; Garcia, S. R.; Kwok, R. W.; Boscoboinik, A.; Valles, D. J.; Marianski, M.; Martini, A.; Carpick, R. W.; Braunschweig, A. B. Acceleration of Diels-Alder reactions by mechanical distortion. *Science* **2023**, *380*, 1053–1058.

(29) Huang, C.; Katz, H. E.; West, J. E. Solution-processed organic field-effect transistors and unipolar inverters using self-assembled interface dipoles on gate dielectrics. *Langmuir* **2007**, *23*, 13223–13231.

(30) Gutiérrez Moreno, J. J.; Pan, K.; Wang, Y.; Li, W. Computational Study of APTES Surface Functionalization of Diatom-like Amorphous SiO2 Surfaces for Heavy Metal Adsorption. *Langmuir* **2020**, *36*, 5680–5689.

(31) Zhu, W.; Zheng, G.; Cao, S.; He, H. Thermal conductivity of amorphous SiO2 thin film: A molecular dynamics study. *Sci. Rep.* **2018**, *8*, 10537.

(32) Hanwell, M. D.; Curtis, D. E.; Lonie, D. C.; Vandermeersch, T.; Zurek, E.; Hutchison, G. R. Avogadro: an advanced semantic chemical editor, visualization, and analysis platform. *J. Cheminform.* **2012**, *4*, 17.

(33) Martínez, L.; Andrade, R.; Birgin, E. G.; Martínez, J. M. PACKMOL: a package for building initial configurations for molecular dynamics simulations. *J. Comput. Chem.* **2009**, *30*, 2157–2164.

(34) Plimpton, S. Fast Parallel Algorithms for Short-Range Molecular Dynamics. *J. Comput. Phys.* **1995**, *117*, 1–19.

(35) Soria, F. A.; Zhang, W.; van Duin, A. C. T.; Patrito, E. M. Thermal Stability of Organic Monolayers Grafted to Si(111): Insights from ReaxFF Reactive Molecular Dynamics Simulations. *ACS Appl. Mater. Interfaces* **2017**, *9*, 30969–30981.

(36) Evans, D. J.; Holian, B. L. The Nose–Hoover thermostat. *J. Chem. Phys.* **1985**, *83*, 4069–4074.

(37) Stukowski, A. Visualization and analysis of atomistic simulation data with OVITO–the Open Visualization Tool. *Modell. Simul. Mater. Sci. Eng.* **2009**, *18*, 015012.

(38) Jas, G. S.; Wang, Y.; Pauls, S. W.; Johnson, C. K.; Kuczera, K. Influence of temperature and viscosity on anthracene rotational diffusion in organic solvents: Molecular dynamics simulations and fluorescence anisotropy study. *J. Chem. Phys.* **1997**, *107*, 8800–8812.

(39) Lecot, S.; Lavigne, A.; Yang, Z.; Géhin, T.; Botella, C.; Jousseaume, V.; Chevolot, Y.; Phaner-Goutorbe, M.; Yeromonahos, C. Arrangement of Monofunctional Silane Molecules on Silica Surfaces: Influence of Alkyl Chain Length, Head-Group Charge, and Surface Coverage, from Molecular Dynamics Simulations, X-ray Photoelectron Spectroscopy, and Fourier Transform Infrared Spectroscopy. *J. Phys. Chem. C* **2020**, *124*, 20125–20134.

(40) Roscioni, O. M.; Muccioli, L.; Mityashin, A.; Cornil, J.; Zannoni, C. Structural Characterization of Alkylsilane and Fluoroalkylsilane Self-Assembled Monolayers on SiO2 by Molecular Dynamics Simulations. *J. Phys. Chem. C* **2016**, *120*, 14652–14662.

(41) Ghorai, P. K.; Glotzer, S. C. Molecular Dynamics Simulation Study of Self-Assembled Monolayers of Alkanethiol Surfactants on Spherical Gold Nanoparticles. *J. Phys. Chem. C* **2007**, *111*, 15857–15862.

(42) Aldagari, S.; Hung, A. M.; Shariati, S.; Faisal Kabir, S. K.; Ranka, M.; Bird, R. C.; Fini, E. H. Enhanced sustainability at the bitumen-aggregate interface using organosilane coating technology. *Construction and Building Materials* **2022**, *359*, 129500.

TOC Graphic